Materials Science Forum Vols. 697-698 (2012) pp 13-18

doi:10.4028/www.scientific.net/MSF.697-698.13

Prediction of the Hardened Layer in Traverse Cylindrical Grinding-hardening

T. Nguyen[a], L.C. Zhang[b]

School of Mechanical and Manufacturing Engineering
The University of New South Wales, NSW 2052, Australia

[a]thai.nguyen@unsw.edu.au, [b]liangchi.zhang@unsw.edu.au

Keywords: Grinding-hardening, Traverse cylindrical grinding, Temperature field, Moving heat source, Heat source trajectory

Abstract. A finite element heat transfer model incorporating a moving heat source has been developed to predict the temperature field in traverse cylindrical grinding. The model was then applied to analyse the grinding-hardening of quenchable steel 1045. It was found that in the region where the grinding wheel had an entire contact with the workpiece, material would experience a heating-cooling cycle, enabling the generation of a uniform hardened layer. In the transient regions at the two ends of the workpiece where the wheel-workpiece contacts were partial, the material was not hardened but experienced an annealing process. The results were in good agreement with the experimental observations.

Introduction

Grinding-hardening is a technology that uses the heat generated in grinding to create a hardened surface layer by promoting the phase transformation in the components of some types of steel subjected to grinding. The material hardened in this way has a remarkable improvement in wear and fatigue resistances [1-2].

The kinetics of phase transformations in such steel depends greatly on the temperature and time during a heat treatment process [3]. Unlike the conventional heat treatment processes where the heating-cooling cycles can be relatively easily controlled, it is complex in grinding. The grinding heat source is generated within a small wheel-workpiece interaction zone. Depending on the grinding methods, this heat source will move on the grinding surface at different trajectories. In traverse cylindrical grinding, the heat source follows two motions: one is a rotation about the cylinder axis and the other is in the longitudinal feed direction. While the heat source is moving, the material in its vicinity experiences convective cooling. Therefore, the control and selection of the grinding parameters to obtain a desired hardened layer and micro-structure rely on a comprehensive understanding of the temperature field during this transient heat transfer process. The heat transfer analysis of grinding to date, however, is limited to surface grinding [4] or to plunge cylindrical grinding [5].

This study aims to understand the heat transfer process in traverse cylindrical grinding and to predict the hardened layer developed with the aid of the finite element method.

Modelling

The calculation of the temperature field was based on a 3D unsteady-state heat conduction equation, applying on a cylinder (Fig. 1):

$$\frac{1}{r}\frac{\partial}{\partial r}\left(kr\frac{\partial T}{\partial r}\right)+\frac{1}{r^2}\frac{\partial}{\partial \theta}\left(k\frac{\partial T}{\partial \theta}\right)+\frac{\partial}{\partial z}\left(k\frac{\partial T}{\partial z}\right)+\dot{q}_g=\rho C_p\frac{\partial T}{\partial t}. \quad (1)$$

where $\dot{q}_g$ is the heat rate per unit volume during phase transformation [4-5], k is the thermal conductivity, ρ is the density and C_p is the specific heat. The dependence of thermal properties (k, ρ and C_p) on temperature of the workpiece material, steel 1045 in this study as has been listed in Refs. [4-5], was incorporated in the finite element computation using ANSYS. Eq. (1) was solved by applying the following initial and boundary conditions:

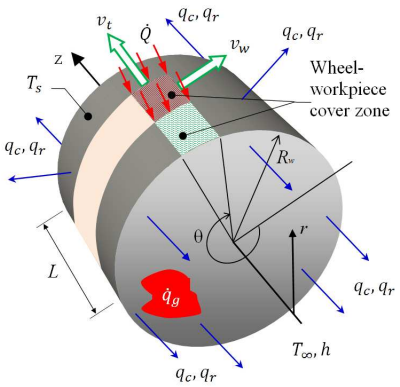

Fig. 1. Thermal conduction in a workpiece.

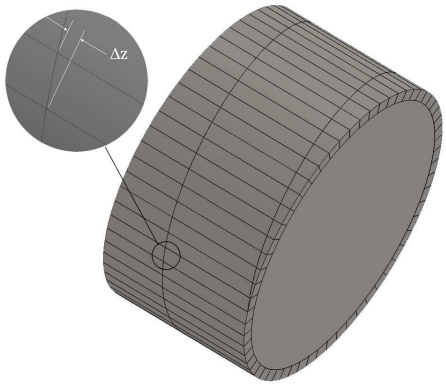

Fig. 2. Surface meshing.

Initial conditions

$$T(r,z,t)\big|_{t=0} = T_\infty = 22^o C, 0 \le r \le R_w \text{ and } 0 \le z \le L \,. \tag{2}$$

where T_∞ is the ambient temperature, R_w and L are the initial radius and length of the workpiece cylinder, respectively.

Boundary condition for heating – moving heat source. The grinding heat can be regarded as a heat flow sweeping on the peripheral workpiece surface with the same velocity as that of the workpiece but in opposite direction. In traverse cylindrical grinding, there are two motions of the workpiece: one is a rotation about the workpiece axis with angular velocity ω_w and the other is a linear motion longitudinal to the machined surface with a feed rate v_t. The equations of motion can be derived in the parametric form as

$$\begin{cases} \theta(t) = \omega_w t = \dfrac{v_w}{R_w} t & t = 0,\ \theta(t) = 0 \\ z(t) = v_t t & t = 0,\ z(t) = 0 \end{cases} . \tag{3}$$

where v_w is the tangential velocity of the workpiece; $\theta(t)$ and $z(t)$ are the angular position and total longitudinal feed at time t, respectively.

The workpiece cylinder was meshed with a spiral configuration associated with the motion profile as shown in Fig. 2. The peripheral surface, where the moving heat source was applied, was divided in the circumference with equal N_c divisions and in the longitudinal direction with a step increment of Δz, *i.e.*,

$$\Delta z = \frac{v_t}{v_w} \frac{2\pi R_w}{N_c} . \tag{4}$$

The heat flow $\dot{Q}(t)$ applied on the n^{th} element is derived as

$$\dot{Q}(t) = \begin{cases} \eta u \dot{V}_n & (n\text{-}1)\Delta t \le t \le n\Delta t \\ 0 & t < (n-1)\Delta t \cup t > n\Delta t \end{cases} . \tag{5}$$

where η is the fraction of total energy conducted as heat into the workpiece (heat partition ratio), determined according to Refs. [4-5]; u (J/mm^3) is the specific grinding energy which can be determined based on the correlated data from Refs. [5-8]:

$$u = 61.64 \dot{V}''^{-0.176} = 61.64 \left[v_w a \frac{(2R_w - a)}{2(R_w - a)} \right]^{-0.176} . \tag{6}$$

in which $\dot{V}''$ ($mm^3/mm.s$) is specific material removal rate per unit wheel width; a is the depth of cut; and Δt is the time required for the heat source moving in a step increment Δz, *i.e.*,

$$\Delta t = \frac{2\pi R_w}{N_c v_w}. \tag{7}$$

The volumetric material removal rate associated with the n^{th} element ($\dot{V}_n$) is determined by

$$\dot{V}_n = \frac{\pi}{N_c \Delta t}[R_w^2 - (R_w - a)^2]\bar{l}_n. \tag{8}$$

Rearranging Eqs. (5), (7) and (8) gives

$$\dot{Q}(t) = \begin{cases} \eta u v_w a\left(1 - \frac{a}{2R_w}\right)\bar{l}_n & (n\text{-}1)\Delta t \le t \le n\Delta t \\ 0 & t < (n-1)\Delta t \cup t > n\Delta t \end{cases}. \tag{9}$$

The average ground width of the n^{th} element ($\bar{l}_n$) can be derived as follows.

During the first and the last revolutions of the workpiece, the grinding wheel does not contact with the workpiece entirely by its width. The ground width varies continuously:

- For the 1st revolution ($n \le N_c$): $\bar{l}_n = (n - 0.5)\Delta z$, (10)
- For the last revolution ($n \ge L/N_c$): $\bar{l}_n = \left(\frac{L}{\Delta z} + N_c + 0.5 - n\right)\Delta z$. (11)

To ensure that the entire workpiece surface is ground by a grinding wheel of width B, the feed rate and the workpiece speed (v_w) are selected so that:

$$z\big|_{\theta=2\pi} = 2\pi R_w \frac{v_t}{v_w} \le B. \tag{12}$$

The inequality sign in Eq. (12) is associated with the case that for ($L/\Delta z > n > N_c$) there is a zone where the wheel surface overlaps with the surface ground from a previous revolution of workpiece. In this zone, the wheel surface does not mechanically interact with the workpiece surface to generate heat. As a result, although the total longitudinal feed *z(t)* increases during the operation, the average ground width maintains as a constant, *i.e.*

$$\bar{l}_n = N_c \Delta z, (L/\Delta z > n > N_c). \tag{13}$$

Boundary condition for cooling

$$-k\frac{\partial T}{\partial \vec{n}} = q_c + q_r = h(T_s - T_\infty) + \varepsilon\sigma(T_s^4 - T_\infty^4). \tag{14}$$

where $\vec{n}$ is the unit vector normal to the surface of a boundary; q_c and q_r are the surface heat fluxes associated with the convective cooling and radiation, respectively; T_s is the surface temperatures; σ is the Stefan-Boltzmann constant ($5.67\times10^{-8} Wm^{-2}K^{-4}$); and ε is the emissivity of the steel workpiece material ($\varepsilon = 0.21$ [9]).

The convective heat transfer coefficient, h applied on the surface normal to the two sides of the cylinder $\vec{n}_z$ and $-\vec{n}_z$ is

$$h\big|_{z=0} = h\big|_{z=L} = h_a. \tag{15}$$

where h_a is the heat transfer coefficient due to air flow.

On the cylindrical surface of the workpiece, the area exposed to the ambient, *i.e.*, that outside the wheel-workpiece interaction zone (Fig. 1), is also subjected to convective cooling. This area *A(n)* can be determined as

$$A(n)=\left\{\sum_{i=1}^{N}A_i\right\}\setminus\left\{\sum_{k=0}^{K}A_{n-kN_c}:[z(n)-z(KN_c]\le B\right\}. \tag{16}$$

where $\left\{\sum_{i=1}^{N}A_i\right\}$ is the peripheral surface area of the workpiece cylinder in which N is the total number of elements; $\left\{\sum_{k=0}^{K}A_{n-kN_c}:[z(n)-z(KN_c)]\le B\right\}$ is the wheel-workpiece interaction zone; and $z(n)$ and $z(KN_c)$ are the longitudinal feeds associated with the elements n and KN_c, respectively.

The heat transfer coefficient applied on $A(n)$ is determined as

$$h(t)=\begin{cases}0, & (n\text{-}1)\Delta t\le t\le n\Delta t\\ h_a, & t<(n-1)\Delta t\cup t>n\Delta t\end{cases}. \tag{17}$$

The heat transfer coefficient due to air flow, h_a, can be estimated following the Hilbert's empirical relation for a circular cylinder with radius R_w subjected to a cross flow of air [9]:

$$Nu=\frac{2h_aR_w}{k_a}=CRe^mPr^{1/3}, \tag{18}$$

$$\begin{cases}4\times10^3<Re=\dfrac{2v_sR_w}{\upsilon}<4\times10^4:C=0.193,m=0.618\\ 4\times10^3\le Re<4\times10^6:C=0.027,m=0.805\end{cases}.$$

in which k_a and υ is the thermal conductivity and viscosity of air, respectively; Nu, Pr and Re are the Nusselt, Prandtl and Reynolds numbers, respectively.

The thermal properties of air (k_a, υ and Pr) are functions of temperature and are considered at the film temperature, $T_f=0.5(T_s+T_\infty)$. Within the range of 22°C to 1,495°C (melting temperature of the workpiece material), h_a is computed as

$$h_a=187.3(T_s+T_\infty)^{-0.128}. \tag{19}$$

where h_a is in W/m^2K, T_s and T_∞ are in Celsius degree and $T_\infty=22^0C$ (initial condition).

Radiation is also applicable for the boundary surface $A(n)$ which is exposed to the ambient, *i.e.*,

$$q_r(t)=\begin{cases}0, & (n\text{-}1)\Delta t\le t\le n\Delta t\\ \varepsilon\sigma(T_s^4-T_\infty^4), & t<(n-1)\Delta t\cup t>n\Delta t\end{cases}. \tag{20}$$

Results and discussion

The grinding conditions used in this study were: alumina grinding wheel 57A60LV with diameter/width = 290 mm/20 mm and speed of 1,750 rpm; working sample of 1045 steel with R_w/L = 20 mm/21 mm, work speed v_w = 40 rpm, feed rate v_f = 8.4 mm/s, and depth of cut a = 0.127 mm.

Fig. 3 shows the simulation result of temperature field developed in the workpiece. The field was in spiral shape associated with the trajectory of the heat source sweeping on the peripheral workpiece surface. While the heat source was moving, the highest temperature rise was within the wheel-workpiece contact zone. The highest temperature was on the surface as shown in the section A-A.

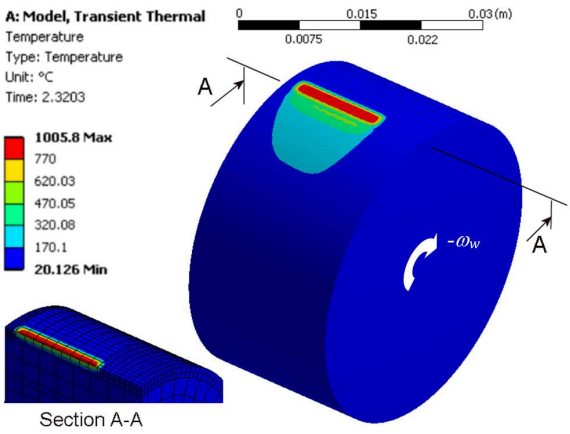

Fig. 3. Temperature field.

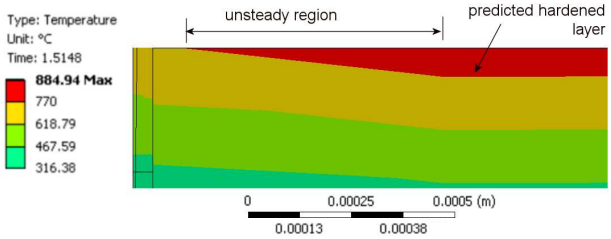

(a). Prediction

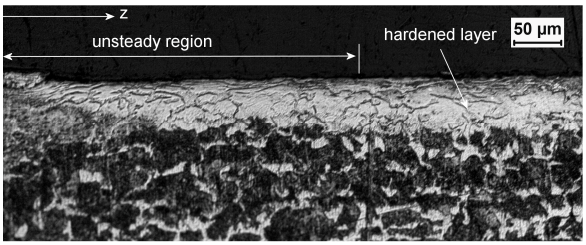

(b). Experimental result

Fig. 5. Variation of the hardened layer thickness along z-direction, θ (rad) = θ (rad) = (2 + 1/60)π

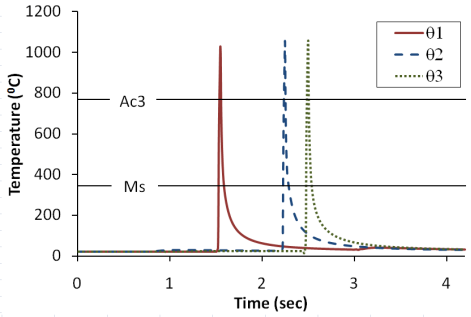

(a). z = 10.5mm

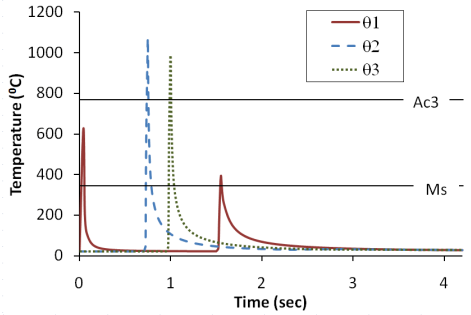

(b). z = 0.5mm

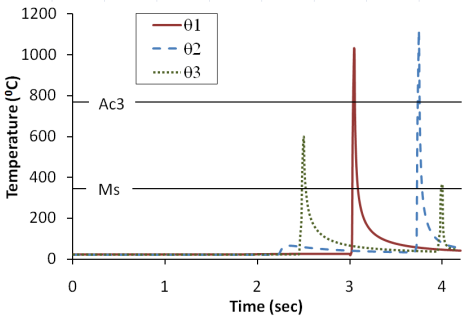

(c). z = 20.5mm

Fig. 4. Temperature history (θ_1 (rad) = π/60, θ_2 = π and θ_3 = (1 + 19/60)π).

Fig. 4 shows the temperature history developed on the ground surface. The development of a hardened layer in steel is a result of phase transformations, where the steel is heated to a temperature above the Ac3, held for a sufficient dwell time for the transformation of pearlite to austenite and then rapidly quenched to the Ms temperature [3]. For instance, by rapid heating with a rate of 10^4K/s, the dwell time is only about 10ms [10] and the quenching rate from the Ac3 of 770°C required for the martensitic transformation in the steel 1045 is less than 200 K/s [11]. At the middle of the workpiece (z = 10.5mm), the grinding wheel contacted entirely with the workpiece by the wheel width regardless the positions θ. It is found that in this zone (Fig. 4(a)), the above conditions for the martensitic transformation were satisfied with the peak temperatures reaching at the same value (≈ 1,050°C). These will enable the generation of a hardened layer with uniformity in thickness. It is compared with those obtained from the two ends of the workpiece cylinder, z = 0.5mm (Fig. 4(b)) and z = 20.5mm (Fig. 4(c)). In the regions where the wheel engaged with the workpiece (θ_1, z = 0.5mm) and ceased from the workpiece (θ_3, z = 20.5mm), the peak temperatures were below the Ac3. Material cannot be hardened but experiences an annealing process.

By probing the peak temperature developed at the Ac3 at subsurface distance of the workpiece, the thickness of the hardened layer can be determined. The variation of the hardened layer thickness along the workpiece axis is illustrated in Fig. 5. It is confirmed that up to the distance z < 140 μm, the temperature rise was not sufficient to generate the phase transformation. There was an unsteady

region (z_u) where the hardened layer thickness varied prior to reaching a constant value (δ). The prediction (Fig. 5(a)) shows that z_u = 600 μm and δ = 70 μm agree well with the experimental results (Fig. 5(b)) of z_u = 400 μm δ = 65 μm.

Conclusions

A finite element heat transfer model incorporating a moving heat source has been developed to predict the temperature field in traverse cylindrical grinding. It is concluded that except at the two ends of the workpiece, material underwent a heating-cooling cycle, enabling the generation of a hardened layer with uniform thickness and microstructure. The model provides an insight to the heat transfer mechanism of grinding-hardening in cylindrical workpieces.

Acknowledgements

This project was financially supported by the Australian Research Council.

References

[1] I. Zarudi and L.C. Zhang, J. Mater. Sci. 37(18) (2002), p. 3935

[2] T. Nguyen, I. Zarudi, and L.C. Zhang, Int. J. Mach. Tls. & Manuf. 47(1) (2007), p. 97

[3] H. Bhadeshia: *Bainite in steels - transformations, microstructure and properties* (The University Press, Cambridge 2001)

[4] T. Nguyen and L. Zhang, Int. J. Mach. Tls. & Manuf. 50(10) (2010), p. 901

[5] T. Nguyen and L. Zhang, Int. J. Mach. Tls. & Manuf. 51(4) (2011), p. 309

[6] D.C. Fricker, T.R.A. Pearce, and A.J.L. Harrison, Proc. Inst. Mech. Engrs., Part B: J. Eng. Manuf. 218 (2004), p. 1339

[7] C. Heinzel and N. Bleil, Annals of the C.I.R.P. 56(1) (2007), p. 327

[8] I. Marinescu, M. Hitchiner, E. Uhlmann, W.B. Rowe, and I. Inasaki: *Handbook of machining with grinding wheels* (Taylor & Francis Group, CRC Press. 2007)

[9] F.P. Incropera and D.P. Dewitt: *Fundamentals of heat and mass transfer* (John Wiley & Sons Inc. 1990)

[10] E. Ohmura, K. Inoue, and K. Haruta, JSME Int. J., Series 1: Solid Mechanics, Strength of Materials 32(1) (1989), p. 45

[11] G.E. Totten, M.A.H. Howes, and T. Inoue: *Handbook of residual stress and deformation of steel* (ASM International 2002)